Design and characterization of macroporous alumina membranes for passive samplers of water contaminants.

Victor M. Orera[a,*], Jorge Silva[a], Helena Franquet-Griell [b], Silvia Lacorte[b]

[a] *Instituto de Ciencia de Materiales de Aragón. CSIC-Universidad de Zaragoza. c/Pedro Cerbuna 12, 50009, Zaragoza, Spain.*
[b] *Department of Environmental Chemistry, IDAEA-CSIC. c/Jordi Girona 18, 08034 Barcelona, Spain*

Corresponding author. *E-mail address:* orera@unizar.es

ABSTRACT

Macroporous ceramic membranes with hierarchical pore structure were developed and characterized for the time-integrated analysis of water contaminants. The alumina membranes were boosted to allow a suitable diffusion rate for envisaged applications. Sacrificial fugitives as cornstarch and graphite and partial sintering technique were utilized for the control of pore structure and morphology. The present study includes: (i) Development of ceramic membrane preparation methods based on wet forming techniques and partial sintering in order to control of membrane parameters such as porosity, tortuosity factor and thickness; (ii) Microstructural characterization of the ceramic membranes using two complementary techniques: Hg-porosimetry and SEM; (iii) the diffusion tests performed under laboratory conditions by an innovative, easy and accurate method based in the use of methylene blue ($C_{16}H_{18}ClN_3S$) water solutions as test compound to study the characteristics of ceramic membranes. Using slip casting and partial sintering processing three different Al_2O_3 membrane configurations with high values 34.5, 36.9 and 39.6 vol% of interconnected porosity and 1.75, 1.7 and 1.3 mm thickness were prepared. The pore morphology consisted of spherical cavities of 5-10 μm diameter and small pores of 70-200 nm. This study also gathers the basis for the calculation of diffusion coefficients, membrane geometrical factor and sampling rates using methylene blue water solutions whose concentration can be accurately determined by optical absorption measurements at 664 nm. Diffusion coefficients for methylene blue range from 2.3±0.5E-8 to 3.0±0.5E-8 $cm^2\ s^{-1}$ increasing as connected porosity increases and membrane thickness decreases. The membrane geometrical factors are low, between 0.6 and 1E-02 and Archie's constants large 4.5 to 5.5. This has been associated to the bimodal pore structure with coexistence of large and small pores that may increase the tortuosity factors in membranes. The macroporous ceramic membranes herein developed are suitable for the fabrication of passive samplers aimed at preconcentrating organic contaminants in water.

SHORT ABSTRACT

Macroporous ceramic membranes with hierarchical pore structure were developed and characterized for the time-integrated analysis of water contaminants. The alumina membranes were boosted to allow a suitable diffusion rate for envisaged applications. Sacrificial fugitives as cornstarch and graphite and partial sintering technique were utilized for the control of pore structure and morphology. The present study includes: (i) Development of ceramic membrane preparation methods based on wet forming techniques and partial sintering in order to control of membrane parameters such as porosity, tortuosity factor and thickness; (ii) Microstructural characterization of the ceramic membranes using two complementary techniques: Hg-porosimetry and SEM; (iii) the diffusion tests performed under laboratory conditions by an innovative, easy and accurate method based in the use of methylene blue (C16H18ClN3S) water solutions as test compound to study the characteristics of ceramic membranes.

Keywords: Macroporous Ceramic Membrane; Hierarchical Pore Structure; Al_2O_3; Diffusion coefficient measurement; Passive Sampler.

1. Introduction

Concern on the increasing presence of toxic water contaminants has led to the necessity to develop new monitoring tools. Emerging and priority organic contaminants are found in wastewaters and rivers at concentrations that produce impairment. However, their incidence and real environmental risks are often neglected due in part to sampling difficulties. In order to properly formulate preservation regulations, more information about the presence of these contaminants in the environment is necessary. Environmental monitoring tools require the use of efficient and reliable sampling and analytical techniques that should be straightforward to use, robust and stable under monitoring conditions. Currently, grab sampling is the most common way to monitor surface waters although it might not be completely representative if contamination fluctuates with time. For snap-shot sampling a given volume of water is collected at a given time using bailers or pumps. Limitations to active sampling are well known and have been described elsewhere [1]. Alternatively, passive or diffusive samplers (PS) offer information on average pollution levels over several hours or days [2]. PS devices allow the diffusion of contaminants through the membrane due to the difference in chemical potentials between the external and internal surface of the sampler [3]. A sorbent inside the sampler retains the diffusing species. The device efficiency and performance depends on the characteristics of the membrane as well as the polarity and solubility of the contaminants, the nature of the sampled water and properties of the receiving

phase. The main advantages of this technique are that it provides time-integrated concentration values, providing more descriptive information in environments where the concentration of the contaminants is not constant [1], autonomy as external energy source is not needed and easy use. Several PS devices have been developed and applied for the analysis of contaminants in water [4] at levels between 0.01 and 1200 μg L^{-1}, and thus, represent a valid method for water monitoring provided they are properly calibrated using controlled conditions.

Ceramic dosimeters were first developed at the University of Tübingen [5] and validated for the analysis of polycyclic aromatic hydrocarbons (PAHs) in groundwater [6,7] and flame retardants in rivers [8]. They are compact, robust, portable and inexpensive and offer information on average pollution levels from few hours to months. They do not require supervision and can be used in hazardous environments. The ceramic dosimeters consist of a porous cylindrical permeable ceramic membrane containing an adsorbent inside. After the sampling period, the adsorbed analytes are extracted and analyzed. State of the art ceramic membranes have a configuration of 50 mm of length, 1.5 mm thickness and 10 mm outer diameter and the pore diameter is of 5 nm [6]. Tested for PAHs in groundwater, the flow rate of these ceramic dosimeters was of 1.5-2.5 mL d^{-1}. The same system provided a similar flow rate (0.39-3.7 mL d^{-1}) when used for flame-retardants in surface waters, although fouling was observed after 6 days deployment [8].

This study focuses on the development of a new ceramic membrane for passive sampling where novelty relies in the achievement of pore structures different than that used previously. The motivation is as follow. In the CPS device the water impregnated at the porous ceramic tube acts as a diffusion barrier for the contaminants, which are thereafter retained by the adsorbent or receiving phase. Since the flow of contaminants and the accumulation in the receiving phase depends on the chemical gradient and the diffusivity of the pollutants through the membrane, there is a critical dependence of the device performance on the membrane structure. In particular, porosity, inertness, mechanical resistance, pore size and diffusion length are the key parameters defining the ceramic membrane. Preferentially, pore volume should be large enough to retain high water volumes also aiming to decrease the unwanted effect of interaction of solute molecules with the ceramic walls. In addition, good interconnectivity between pores enhances solvent diffusion but pore size has to allow capillarity forces to keep the water in the membrane ceramic walls avoiding swelling effects and water flux. Furthermore, the matrix material has to be chemically and mechanically stable for long deployment times in natural waters. The membrane has to present enough robustness to resist tight sealing, water turbulences, etc.

All these requirements can be achieved through appropriate choice of materials and forming techniques but keeping in mind the industrial scalability and final price of the device. In this work we produced monolithic ceramic membranes of Al_2O_3 with a combination of macro-pore morphologies using sacrificial pore former phases and partial sintering techniques. These porous ceramics are referred to as materials with hierarchical porosity. The fabrication and properties of ceramics with hierarchical porosity has been extensively described in some reviews [9]. To better understand the role of pore structure and membrane dimensions on the up-taking ratio of the CPS, three sets of macro-porous ceramic membranes with different bimodal distribution of pores and membrane thickness were prepared and were calibrated for the time-weighted average determination of contaminant concentrations in water. Their performance was tested using methylene blue water solutions as test compound that allow us to determine some useful membrane parameters such as diffusivity, sampling rate, tortuosity, etc.

2. Experimental

2.1. Materials and fabrication methods.

Fig. 1. CPS device fabricated with the ceramic membranes described in this paper.

Figure 1 shows a CPS sampler fabricated with one of the ceramic membranes studied in this paper. Observe the rubber caps closing the inner membrane volume where concentrator is placed. The ceramic membranes were fabricated by slip casting method. This is a relatively cheap and reproducible method suitable for large-scale production of nearly to

final shape green ceramics. Critical aspect of the fabrication process is the preparation of ceramic suspensions. Ceramic suspensions were prepared using aluminum oxide powders (α-Al2O3, Ceralox APA-0.5, 8.1 m^2/g, Sasol North America, Inc., grain size D_{50} = 300 nm) and water. Suspensions were stabilized using Duramax D-3005 as dispersant (1% in solid weight). Two stable suspensions CP1 and CP2 with different sacrificial phases as pore generator agents, cornstarch or cornstarch and graphite (Alfa Aesar, 325 mesh, 44 μm, 99.9%), were prepared. Suspension compositions are given in Table 1. The morphology of starch powders used in this work has been recently published [10]. They present irregular prismatic shapes with a relatively narrow particle size distribution D_{50} = 10 μm as measured by laser diffraction in a Mastersizer 2000 equipment. The rheology of suspensions was controlled to achieve the optimum processing conditions. In particular the composition of the colloids was adjusted to get a viscosity for proper filling of mold without entrapping of air bubbles.

Table 1.

Suspension composition in weight %.

	CP1	CP2
Al_2O_3	58.5	58.0
Water	29.25	27.2
Graphite	0	2.8
Cornstarch	12.25	12
Sacrificial phase volume (%)	37	40

The volume of the solid organic phases was calculated using the following solid phase density values: alumina density 3.98 g cm^{-3}, starch density 1.43 g cm^{-3} and graphite density 2.16 g cm^{-3}. Dispersant and water solvent were first mixed by magnetic stirring for 15 min. Alumina powders and pore formation agents were poured into the mix and stirred for 30 min. The resulting paste is treated with ultrasounds for 1 minute and magnetic stirred again for 30 min. The stable ceramic paste was poured in a plaster mold with the desired cylindrical geometry. The time that the suspension remains in the mold determines the thickness of the raw piece, and the composition of the suspension determines its porosity and microstructure. After casting the green membranes were pre-sintered in air at 950ºC for 4 hours and gently rectified and polished. Thermogravimetric analysis (TGA) confirmed that all organics have been burnt out at temperatures above 560ºC. The membranes were partially sintered at 1300ºC for 3 hours dwelling time and heating and cooling rates of 2ºC min^{-1}.

Three different membrane families were made. Two thicker membranes, 1.75 mm thickness, MCPS1 and MCPS2 were prepared with pastes CP1 and CP2 respectively and permanence on mold times of 12 min. A thinner membrane, 1.3 mm thick, MCPS3 was fabricated with paste CP2 and permanence time of 6 min. The dimensions are specified in Table 2. All the membranes have the same length, about 50 mm, but as the sealing caps fill part of the cylinder inner space the inner membrane volume occupied by liquid was determined measuring the extracted liquid volume. Inner volume is the same for MCPS1 and MCPS3, about 3.5-3.6 mL, and smaller, 2.7 mL in MCPS2 membranes. The external radius of the cylinders is determined by the slip casting mold dimensions and the contraction during sintering. It ranges between 7.1 and 7.35 mm.

Table 2.

Dimensions and porosity values of the ceramic membranes.

	MCPS 1	MCPS 2	MCPS 3	Ref. [6]
Length (mm)	50±2	50±2	50±2	50
Density (g/cm^3)	2.37	2.30	2.38	-
External diameter (mm)	14.6±0.3	14.15±0.35	14.7±0.2	7
Thickness (mm)	1.75±0.2	1.7±0.17	1.15±0.05	1.5
Pore size (nm)	80; 2000	100; 2000	100; 3000	5
Total porosity (%)*	40	42	40	-
Connected porosity (%)	34.5	36.9	39.6	30.5%

* Calculated from comparison between measured ceramic density and dense alumina density

- not indicated

2.2. Microstructure characterization

The microstructure of the porous ceramic was studied in polished transverse membrane cross-sections using a JEOL 6301F scanning electron microscope (SEM). The SEM specimens were embedded in epoxy resin and polished in cross-sections according to a polishing procedure previously published [11]. Open and connected porosity was measured by means of an Hg porosimeter (Poremaster, Quantachrome; maximum pressure 30,000 psia). Total porosity was determined by gravimetric density measurement.

2.3 Diffusion test

To test the performance of the cylindrical ceramic membranes and calculate the sampling rates of the device we used a water solution of methylene blue ($C_{16}H_{18}ClN_3S$) as model compound because it is a stable solution, it gives intense color when diffuses into the porous membrane giving information about homogeneity in pore structure, presence of cracks or other structural defects and its concentration can be accurately computed by measuring the optical absorption spectra. The absorption of methylene blue solutions was measured in an HP-Agilent 8453 (Agilent Technologies, CA, USA) spectrophotometer with a diode array detector (DAD). The value of the absorbance at 664 nm, which corresponds to the maximum of one absorption band of this compound, was used as an accurate measure of the concentration. In figure 2 we give the spectroscopic calibration of several solutions of methylene blue giving a molar extinction coefficient of 6.4 ± 0.05 x 10^4 $cm^{-1}M^{-1}$ for the measurement conditions used here.

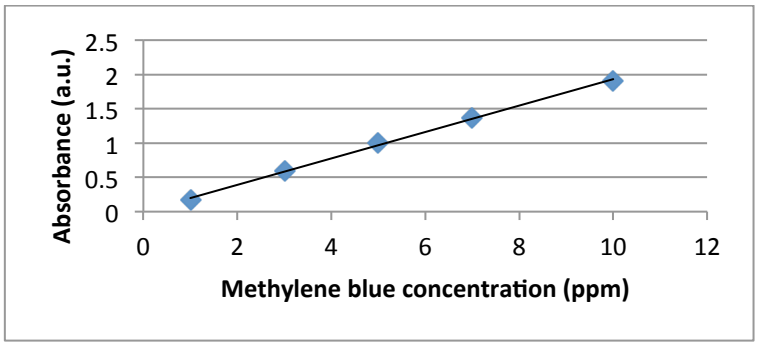

Figure 2. Methylene blue spectroscopic calibration curve used in this study. Optical absorption of $C_{16}H_{18}ClN_3S$ solutions at 664 nm as a function of concentration.

Using methylene blue dye and the optical absorption technique we studied the water solution diffusion through the membranes. A beaker with 4 L of mineral water was dosed with methylene blue at 10 mg L^{-1}. This concentration was used in the optimization protocol as it shows an intense blue color and it can be accurately measured. Several identical cylinders saturated with clean water to create the water membrane were placed in the methylene blue solution. The membranes were closed with thermoplastic rubber caps, placed in a handmade support made of tulle net and then placed inside the methylene blue solution. After each exposure period (2, 5, 6, 9 and 12 d), the solution inside the sampler corresponding to the different experiments performed, was collected with a Pasteur pipette and placed in a glass vial. Measuring the concentration of methylene blue inside the sampler as a function of the exposure time permits to establish the flow and diffusion rates of membranes. The external solution from the beaker was also monitored to control the stability of methylene blue

throughout the deployment time. To quantify the concentration of methylene blue inside the cylindrical membranes, we used the calibration values given above.

2.4 Theory and data calculation

Analysis of the MCPS up-takings yielded the accumulated mass of solute $M_s(t)$ diffused through the cylindrical membrane surface over the sampling time *t*. If during the sampling period the mass flow of contaminants across the water membrane is diffusion limited and diffusion is radial (long cylinder approach) the concentration is only function of radius r and time t. The diffusion equation is [12].

$$\frac{\partial C}{\partial t} = \frac{1}{r}\frac{\partial}{\partial r}\left(rD_e\frac{\partial C}{\partial r}\right) \quad (1)$$

where D_e is the effective diffusion coefficient of solute in solvent, measured in cm^2s^{-1} and stands for the diffusion of analytes through the water filled porous ceramic membrane. $\frac{\partial C}{\partial r}$ is the concentration gradient [13].

Consider a cylindrical membrane of inner and outer radii *a* and *b*. If the concentration inside cylinder is maintained close to zero, for example if a sorbent is used, and the matrix solute concentration $C(b)=C_0$ is constant, the steady state mass flux at $r=a$ is proportional to the concentration gradient. The accumulated solute mass $M_s(t)$ depends linearly on time. It can be given by:

$$M_s(t) = \frac{2\pi LD_eC_0}{\ln(b/a)}.t = k.t \quad (2)$$

where *L* is the sampling cylinder length and the slope of gives the uptake rate, $k(M/t)$ that is directly related with the sampling rate, $R_s(V/t)$. Linear up taking dynamics are usually observed in PS devices.

In the absence of any concentrator the analyte concentration inside the closed cylinder will increase and the concentration gradient will decrease with deployment time. Since the solution of the diffusion equation for a hollow cylinder in the non-steady state is rather complicated we have used that of a solid cylinder instead. The approach could be justified as any mass exchange with the exterior is only made through the membrane wall. Actually, the solution of the diffusion equation for a solid cylinder of infinite length and it has been previously applied, for example, to the study of the reduction kinetics of ceramic composites with cylindrical shape [14,15].

For the solid cylinder, if the diffusion coefficient is constant for initial concentration inside the membrane zero and if L>>b the solution for Eq. (1) is given by Eq. 5.22 in reference [12]

$$\frac{C(a,t)}{C_0} = 1 - \frac{2}{b}\sum_{n=1}^{\infty} \frac{exp(-D_e \alpha_n^2 t) J_0(a\alpha_n)}{\alpha_n J_1(b\alpha_n)} \quad (3)$$

where $J_i(x)$ are the Bessel functions of the first kind and $b\alpha_n$ the positive roots of $J_0(x)$. α_n is given in cm^{-1} units.

3. Results

3.1. Physical characteristics of the membranes

Three porous ceramic membranes were prepared with two different pore former compositions (see section 2.1 and table 2). SEM studies indicate that the morphology of the pore microstructure is essentially the same in the three cases. Figure 3 shows a typical SEM image of a MCPS2 ceramic membrane transverse cross-section where both cornstarch and graphite pore formers were used. A homogeneous and continuous distribution of spheroid cavities around 10 μm diameter through all the membrane depth is observed.

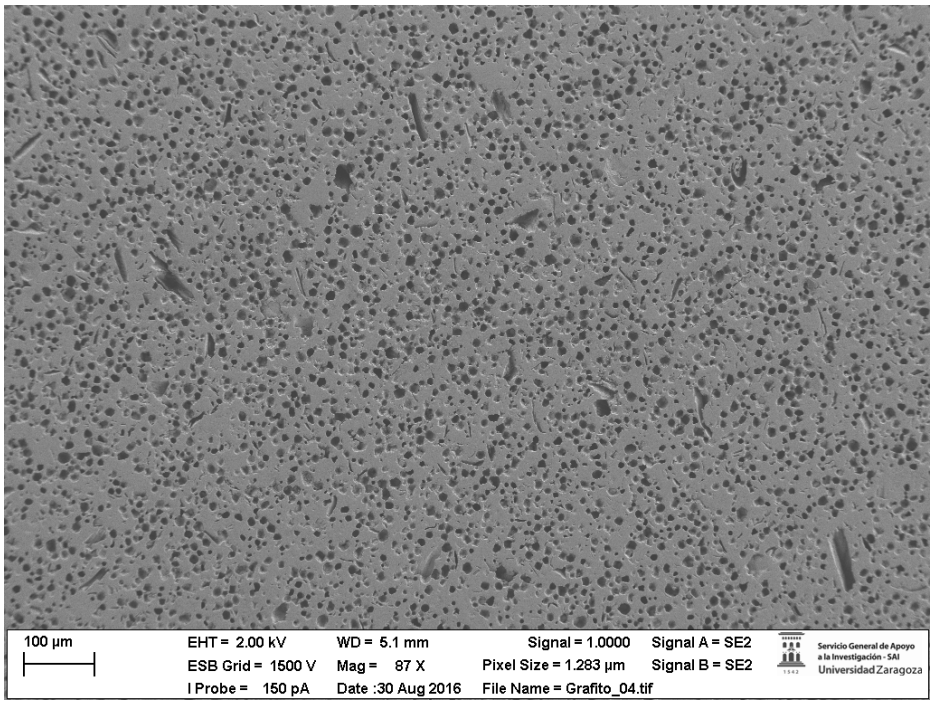

Figure 3. SEM image of the transverse section of a MCPS2 ceramic cylinder showing the pore microstructure.

Figure 4 shows the detailed image of the connecting contact area or necks between cavities. Effect of partial sintering on alumina microstructure can also be seen. Polygonal

alumina grains indicate that strong struts have been produced but leaving some intergranular porosity. This porosity is a consequence of partial sintering and it is related with the alumina grain size being 2 to 5 times smaller than alumina grains in agreement with conventional sintering theories [16].

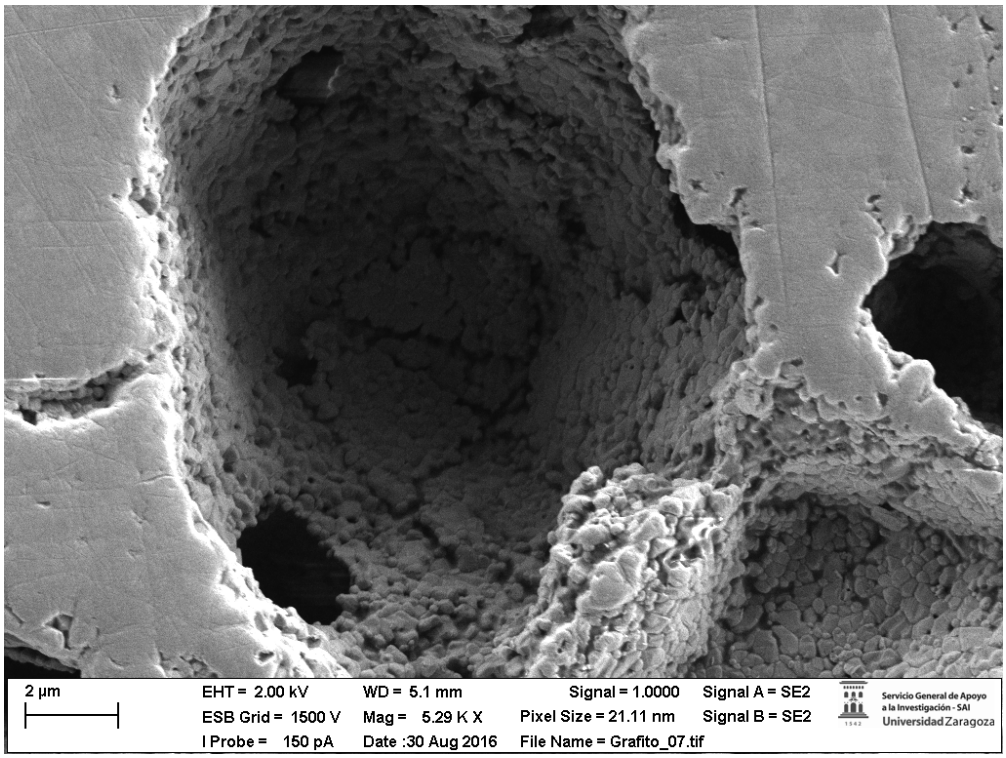

Figure 4. SEM image showing the detail of the cavity and grain structure.

Total porosity of the membrane estimated through density measurements is of around 40% (see table 2) in fair agreement with the volume of sacrificial phase (table 1) indicating that most of pore volume is produced by pore former phase. However, this relatively high porosity value does not endanger the mechanical stability of the membranes that can be safely handled and sealed. On the other hand, as the diffusion of analytes takes place through the connected pore network and closed pores or blind pores do not contribute to transport of matter it is crucial to know the amount of connected pores. The connected pore volume and pore size has been measured using Hg porosimetry. In these measurements, the intruded mercury volume is obtained as a function of the liquid (mercury) pressure (see figure 5).

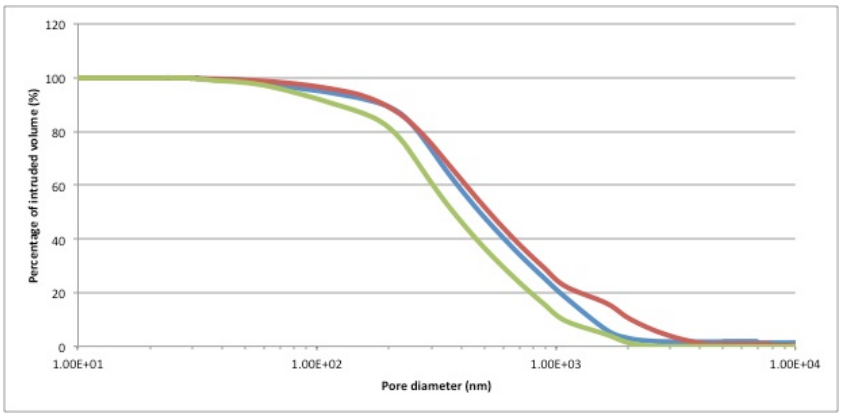

Fig. 5. Percentage of intruded volume as a function of pore diameter as measured by Hg porosimetry. Green, MCPS1; Blue, MCPS2; Red, MCPS3

Due to the capillarity effect the mercury pressure needed to intrude a given cavity is directly related with the size of conduits connecting the pores [17]. However, it has to be taken into account that mercury porosimetry also has some limitations. It provides values of the diameter of the entrance to a pore not of the pore size itself. Also blind holes connected to external surface can be intruded then measured by porosimetry, even if they are not connected to the pore network. Thus, values of connected pores could be overestimated in these measurements, which can be more important for the thinner samplers. Data on total and open porosity obtained as indicated above for the three studied cases are compiled in table 2.

3.2. Testing and calibration of the membranes

As indicated in section *2.3*, the analyte permeation and diffusion rates were studied using methylene blue solution as standard. Two membranes of each configuration (table 2) were placed in the methylene blue solution during 6 days. During exposure period, the 4 L beaker was placed in an orbital shaker (KS500, Janke&Kunkel, IKA WERK, Staufen, Germany) with a constant temperature of 22-23ºC. The orbital shaker has a circular shaking motion at low speed (100 rpm), which does not create vibrations nor produce heat, and it was used to induce a liquid movement simulating the circulating water in a river or wastewater. To determine the water motion effect, we kept 2 more membranes in the same conditions but without motion. In each condition, the concentration of the methylene blue solution inside and outside the cylinder was measured after 6 d by spectrophotometry using the experimental conditions described in section 2.3. The accumulated mass, among the 3 membrane configurations studied, is given in Figure 6.

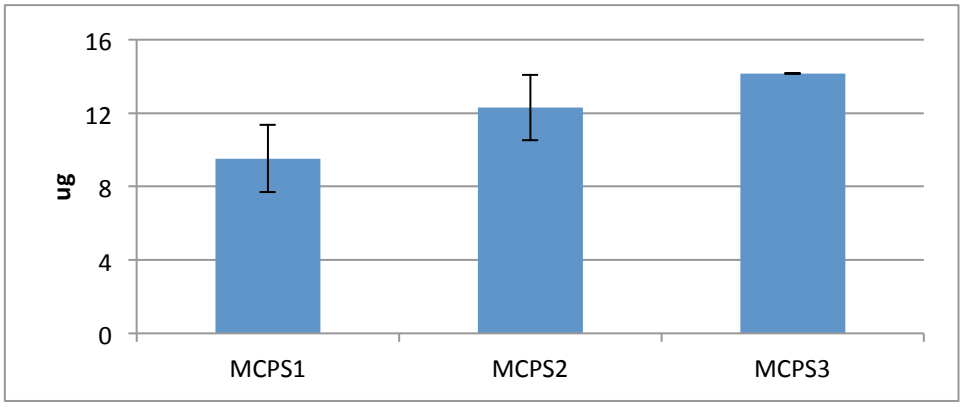

Fig. 6. Total mass of methylene blue accumulated inside the membranes after 6 days of deployment time in a water solution of 8.85 mg/L concentration.

It is observed that the thinner membranes with the highest connected pore volume (MCPS 3) provided the higher accumulation potential at 6 d deployment time. On the contrary the MCPS1 membranes are less efficient although the geometrical parameters are about the same than those of MCPS2 membranes that shows a better performance owing to their higher concentration of connected pores. Motion has not any meaningful effect in the accumulated mass inside the membrane.

To insight the kinetics of mass transport in the membranes the following experiments were performed. Ten MCPS3 cylinders initially filled with clean water were placed inside the methylene blue solution. After 2, 5, 6, 9 and 12 days, two cylinders were removed and the concentration, or accumulated mass of methylene blue inside the cylinder $M_s(t)$ was determined. The concentration in the external solution was also monitored, being C(b)=8.4 ± 0.5 mgL^{-1} nearly constant over time. Because no adsorbent was introduced inside the membrane, the diffusion experiments would correspond to boundary conditions and transport kinetics described by Eq. 3. In figure 7 we plot C(a,t))/C(b) as a function of the sampling time. The data are well fit by Eq. 3 where up to n=8 terms have to be taken to get a good convergence in the series, specifically for the short deployment times. This result justifies "a posteriori" the approach of a transport model based in that of a solid cylinder instead of a hollow cylinder leading to Eq. 3. The best fitting values of D_e are given in table 3. It is interesting to realize that the effective diffusion values obtained with this more accurate model coincide with those calculated from the sampling rate measurements assuming Eq. 2 is valid which only holds for the short deployment times.

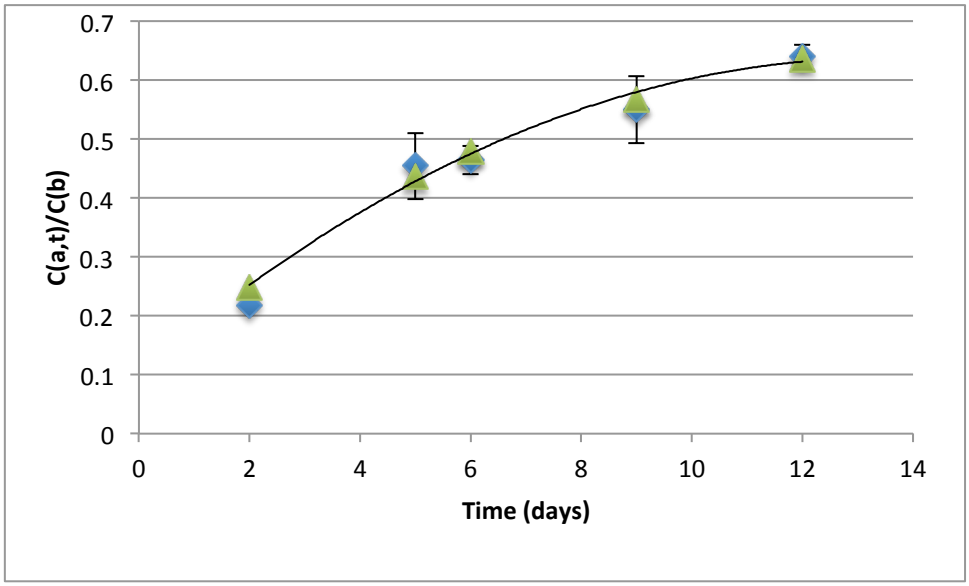

Fig. 7. Ratio of methylene blue concentration accumulated inside the MCPS3 membranes as a function of deployment time. Blue points experimental values, green points calculated values obtained from Eq.3 with effective diffusion coefficient of D_e=3.0 E-8 cm^2/s. Dark line is a best-fit line to theoretical values.

4. Discussion

4.1 Pore structure

The role of the ceramic membrane in the MCPS device is complex. On one side, the porous ceramic holds the water membrane that is actually the diffusion barrier for contaminants transport from the external solution to be monitored to the concentrator confined by the membrane. The ceramic membrane is also the physical container that holds and protects the sorbent material that accumulates the analyte. Consequently, the ceramic microstructure has to be designed to support the largest water volume without weakening the mechanical integrity of the membrane, so that organic contaminants can diffuse across the membrane with minimal interaction with the ceramic material whereas the inner sorbent (diameter >30 μm) does not escape from the cylinder. The ceramic membrane has to be also a barrier for microorganisms and mud entering the inner chamber. In our design, porosity, inertness, pore size and diffusion thickness, which are the key parameters defining the ceramic membrane, were amended. The microstructure of the macro-porous membrane was designed to get a porous ceramic shell with a hierarchical pore structure consisting of relatively large spheroid cavities of about 10 μm diameter connected by smaller pores.

Following current knowledge on macro-porous ceramic processing [18, 9] we used starch as sacrificial template to create the large cavities. Starch pore forming is a low-cost and simple technique appropriated synthesis of macro-porous ceramics with pores of less than 20

μm size, difficult to achieve with other pore forming techniques such as polymer replica, wood replica or direct foaming [19,16]. In particular cornstarch powder was dispersed in the alumina suspension to further processing by wet colloidal route using slip casting. We have also explored graphite as pore former. The procedure we used to incorporate graphite to the alumina suspension is similar to that used with starch. In our case the effect of graphite former simply adds to that of starch. The organics including pore former were smoothly removed from the green body by pyrolysis treatment. Any cracking effect in the ceramic was observed. In SEM images the spheroidal cavities resulting from pore formers are clearly seen (figs. 3 and 4). Also Hg-porosimetry results (fig. 5) show the presence of a large amount of pores with sizes between 200 to 2000 nm that could be associated to the entrances to spheroidal cavities as shown in fig. 4. It is interesting to realize that addition of graphite as pore former produces an increase in the size of these pores. Porosimetry measurements show the presence of a small amount of large pores about 5 to 10 μm diameter more evident in samples MCPS1 and MCPS3 in fig. 5 that could be associated either to cavities with large entrances or to cavities at the membrane surface. To increase connectivity between cavities small inter-cavity channels were produced using partial sintering conditions. These small pores can be seen in the SEM images at the grain boundaries of alumina grains (see fig. 4). According to porosimetry results (fig. 5) there contribution to the total pore volume is modest, less than 10% volume, but increased pore connectivity. The size of these small pores is between 70 to 200 nm.

Finally, it is interesting to point out that using these suspension compositions and forming procedures there is not any significant dimensional change during drying and demoulding process. The size of spherical pores corresponds to that of starch pore formers indicating that there is not significant swelling or water uptake by starch particles during the process. In fact both starch and graphite are rather insoluble in water at ambient temperatures. The open (connected) porosity values of these membranes are quite large ε = 0.345, 0369 and 0.396 for MCPS1, MCPS2 and MCPS3 respectively. In fact, in the case of the thinnest MCPS3 membrane essentially all the pores are accessible to Hg infiltration.

The parameters describing the pore structure of the MCPS used in this study are compared in Table 2 with those of state of art sampler [6]. Main difference between both systems arises in the higher porosity values and much larger pore size in the MCPS membranes studied in this work. As a consequence of this particular microstructure the present MCPS membranes can be easily saturated with large water volumes and the interaction between analyte and pore walls is expected to be minimum. The ceramic membrane thickness is also much larger than the diffusion barrier length of the sampled chemicals that has been estimated by Gale of the order of 100 to 400 nm [20]. In addition, the size of pores is small

enough to avoid microorganisms entering the dosimeter and any net flow of water. As a consequence we expect that the mechanism governing the contaminants transport through the membrane is in our case a true diffusion rate-limiting process and data can be analyzed using ad hoc diffusion theory.

4.2 Diffusion of analytes.

Using the data given in fig. 6 the uptake rates for sampling times of 6 days were calculated assuming a linear dependence with deployment time as predicted by Eq. 2. Taking into account the concentration of external solution we calculated the sampling rates for methylene blue that are given in table 3. As expected the sampling rates are modest, as any concentrator is used in this experiment, but clearly show the increases through the MCPS1, MCPS2 and MCPS3 sequence. At a first sight and according to porosity values in table 2 it could be concluded that sampling rates increases with membrane porosity. However, sampling rates also depend on membrane geometrical factors such as thickness and inner volume.

Table 3. MCPS membrane characterization parameters: D_e, effective diffusion coefficient; D_w, diffusion coefficient in water (theoretical estimation); *F*, membrane geometrical factor; *m*, Archie's exponent value; R_s, sampling rate; and uptake rate; *k*.

	k (μg day^{-1})	R_s (mL day^{-1})	D_e (Eq. 2) (cm^2 s^{-1})	D_e (Eq. 3) (cm^2 s^{-1})	*F*	*m*
MCPS1	1.6	0.18	2.3±0.5E-8		1±0.5E-2	4.5±0.5
MCPS2	2.05	0.23	2.9±0.5E-8		0.75±0.1E-2	4.9±0.1
MCPS3	2.4	0.27	2.7±0.1E-8	3.0±0.5E-8	0.6±0.1E-2	5.5±0.1

The dependence of sampling rates in the membrane geometrical factors can be eliminated if the effective diffusion parameter through the membrane is calculated. In fact, following previous studies of solute diffusion through porous media [21] it is evident that the effective diffusion parameter D_e is related with the actual diffusion coefficient in water D_w by the membrane geometrical factor *F*.

$$D_e = D_w.F \quad (4)$$

According to Delgado et al., [22]

$$F = \varepsilon.\delta/\tau \quad (5)$$

τ (>1) is the tortuosity factor, a geometrical factor related with the pore geometry, δ (≤1) is the constriction factor assumed to be unity in the present case as the predominant large cavities and wide channels makes collision between molecules much more probable than with the pore walls and ε stands for the value of effective or connected porosity. Alternatively, the

most extensively used relationship to obtain diffusion coefficients of contaminants in water in relation with geometrical factors of the membrane is the Archie´s law [23], typically used by geologists to link the electrical resistivity of a rock to its porosity and to the resistivity of the water that saturates its pores.

$$F = \varepsilon^m \quad (6)$$

Where m is known as the cementation exponent. Both eq. 5 and 6 are equivalent in order to account for the membrane geometrical factor that relates the pore structure with the sampling rates of the MCPS.

The calculation of the effective diffusion coefficient D_e can be done either using the simplest linear time dependence predicted by Eq. 2 or the most accurate model of Eq. 3. It is interesting to notice that Eq. 3 also predicts a linear dependence with time for short deployment times. Using Eq. 2, the geometrical dimensions in table 2, the effective membrane length estimated from the measure of the spiked liquid inside membrane and inner radius and the calculated sampling rates we get a value of the effective diffusion coefficient of methylene blue in those membranes given in table 3. Errors involved in determination of D_e are large owing to the uncertainties in the measure of the accumulation rates. Comparison of MCPS 1 and 2 membranes seems to indicate an increase on diffusion factor in the later, which could be associated with the higher porosity produced by graphite pore formers. However this implementation with increasing porosity has not been seen in the MCPS3 membranes. It might be possible that a part of the measured porosity in the Hg-porosimetry experiments would correspond to near to surface pores that would be isolated from the pore network. In fact, the porosity curves for MCPS2 and MCPS3 in fig. 5 are very similar except for some amount of large cavities that are detected in the MCPS3 membranes and that as it has been pointed out before could correspond to cavities near surface with large entrance pores. We have to realize that MCPS3 membranes are the thinnest ones so with larger surface to volume ratios.

In order to calculate the membrane geometrical factor, F, we can apply eq. 4. We have not found values of diffusion coefficient of methylene blue in water in literature. Consequently, we used the estimated diffusion coefficient in water at room temperature resulting from equation D_w=3.59E-07 T(K)/$M^{0.531}$ that gives a theoretical estimation of the diffusion coefficient of methylene blue in water D_w= 5.1E-06 cm^2s^{-1}. Then, using eqs. 4 and 6 we can obtain the membrane geometrical factors an Archie's exponent values given in Table 3.

In spite of the quite large connected porosity values the membrane geometrical factors are low and the Archie´s coefficients high. That results in high values of the tortuosity factor in these ceramics. Unexpectedly, tortuosity seems to increase with porosity. One possible explanation could be related with the bimodal pore morphology in these ceramics. In

fact it has been reported that a distribution of pores with varying cross sections may cause abnormally high tortuosity factors [24] although, to our best knowledge, this important aspect has not been studied in detail up to now.

However, the pore microstructure developed in these ceramic membranes gives enough uptake capacity and stability for being used in the fabrication of CPS devices for the analysis of organic contaminants in river waters or wastewater. Recently, it has been reported that CPS fabricated with the "a priory" less optimized MCPS1 membranes, were successfully used for the monitoring of cytostatic drugs in water [25]. These devices achieved sampling rates between 0.825 and 3.350 mL day^{-1} that allowed for the first time the detection of cyclophosphamide and mycophenolic acid at concentrations of 19 ± 3 and 136 ± 28 ng L^{-1} in effluent waters of a Waste Water Treatment Plant (WWTP) in Barcelona.

5. Conclusions

Macroporous alumina membranes have been developed. Using pore formers and partial sintering techniques a hierarchical pore morphology consisting of large cavities 5-10 μm diameter and small pores of 70-200 nm provides high pore volume and good connectivity between pores. The diffusion properties and sampling rates of the ceramic membranes were determined using methylene blue as test compound as a function of the connected porosity values, pore former composition and ceramic thickness. Ceramics with greater values of connected porosity give better diffusivities. Thinner membranes give greater sampling ratio values. This pore structure has been proved appropriated for development of passive samplers for detection of low-concentration emergent organic contaminants in water.

ACKNOWLEDGMENT

Financial support from the Spanish Ministerio de Economía y Competitividad under the projects CTM2014-60199-P regarding the monitoring of cytostatic compounds and MAT2015-68078-R for the development of the ceramic membranes is acknowledged. HF acknowledges FPI grant BES-2012-053000. Authors want to thank to Prof. Rodrigo Moreno from ICV-CSIC, for his precious help in paste and sample preparation. V. Pueyo and T. Sala are acknowledged for making the spectroscopic measurements and R. Tauler for the loan of the instrument.

REFERENCES

[1] L. Jones, J. Ronan, B. McHugh, E. McGovern, F. Regan, Emerging priority substances in the aquatic environment: a role for passive sampling in supporting WFD monitoring and compliance. Anal. Methods, 7 (2015) 7976-7984. DOI: 10.1016/j.envpol.2012.08.014.
[2] B. Vrana, I.J. Allan, R. Greenwood, G.A. Mills, E. Dominiak, K. Svensson, J. Knutsson, G. Morrison, Passive sampling techniques for monitoring pollutants in water, TrAC Trends in Analytical Chemistry, 24 (2005) 845-868. DOI: 10.1016/j.trac.2005.06.006.
[3] T. Górecki, J. Namienik, Passive sampling, TrAC, Trends Anal. Chem., 21 (2002) 276-291. DOI: 10.1016/S0165-9936(02)00407-7
[4] G. Ouyang and J. Pawliszyn, Configurations and calibration methods for passive sampling techniques, J. Chromatography A, 1168 (2007) 226-235. DOI: 10.1016/j.chroma.2007.01.133
[5] H. Martin, M. Piepenbrink, P. Grathwohl, Ceramic dosimeters for time-integrated contaminant monitoring, J. Process Anal.Chem., 6 (2) (2001) 68-73
[6] S. Bopp, H. Weiß, K. Schirmer, Time-integrated monitoring of polycyclic aromatic hydrocarbons (PAHs) in groundwater using the Ceramic Dosimeter passive sampling device, J. Chromatogr. A, 1072 (2005) 137-147. DOI: 10.1016/j.chroma.2004.12.049
[7] H. Martin, B.M. Patterson, G.B. Davis, P. Grathwohl, Field trial of contaminant groundwater monitoring: Comparing time-integrating ceramic dosimeters and conventional water sampling, Environ. Sci. Technol., 37 (2003) 1360-1364. DOI: 10.1021/es026067z
[8] J. Cristale, A. Katsoyiannis, C.e. Chen, K.C. Jones, S. Lacorte, Assessment of flame retardants in river water using a ceramic dosimeter passive sampler, Environ. Pollut., 172 (2013) 163-169. DOI: 10.1016/j.envpol.2012.08.014
[9] P. Colombo, C. Vakifahmetoglu, S. Costacurta, Fabrication of ceramic components with hierarchical porosity, J. Mater. Sci. 45 (2010) 5425-5455. DOI: 10.1007/s10853-010-4708-9
[10] B.I. Arias-Serrano, E.M. Sotomayor, A. Várez, B. Levenfeld, H. Monzón, M.A. Laguna-Bercero and A. Larrea, High-performance Ni-YSZ thin-walled microtubes for anode-supported solid oxide fuel cells obtained by powder extrusion moulding, RSC Adv., 6 (2016) 19007-15. DOI: 10.1039/C5RA28183K
[11] S. Serrano-Zabaleta, M. A. Laguna-Bercero, L. Ortega-San-Martin and A. Larrea, Orientation relationships and interfaces in directionally solidified eutectics for solid oxide fuel cell anodes, J. Eur. Ceram. Soc., 34 (2014) 2123-32. DOI: 10.1016/j.jeurceramsoc.2013.06.008
[12] J. Crank, The mathematics of diffusion, Oxford University Press (1975), ISBN 019 8533446
[13] I. B. Huang and S. K. Yen, Diffusion in hollow cylinders for some boundary conditions I. Matematical treatment, Materials Chemistry and Physics 74 (2002) 289-299. DOI: 10.1016/S0254-0584(01)00483-7
[14] M.A. Laguna-Bercero, A. Larrea, J.I. Peña, R.I. Merino and V.M. Orera, Structured porous Ni- and Co-YSZ cermets fabricated from directionally solidified eutectic composites, J. Eur. Ceram. Soc. 25 (2005) 1455-1462. DOI: 10.1016/j.jeurceramsoc.2005.01.025
[15] V. Gil, A. Larrea, R.I. Merino, V.M. Orera, Redox behavior of Gd-doped ceria-nickel oxide composites, J. Pow. Sources 192 (2009) 180-184. DOI: 10.1016/j.jpowsour.2008.12.053
[16] A. R. Studart, U. T. Gonzenbach, E. Tervoort, L. J. Gauckler, Processing routes to macroporous ceramics: a review, J. Am. Ceram. Soc. 89:6, (2006) 1771-1789. DOI: 10.1111/j.1551-2916.2006.01044.x
[17] H. Giesche, Mercury porosimetry: a general (practical) overview, Part. Part. Syst. Charact. 23 (2006) 1-11.
[18] T. Ohji and M. Fukushima, Macro-porous ceramics: processing and Properties, International Materials Reviews, 57:2 (2012) 115-131. DOI: 10.1179/1743280411Y.0000000006
[19] O. Lyckfeldt and J.M.F. Ferreira, Processing of Porous Ceramics by Starch Consolidation, J. Eur. Ceram. Soc. 18 (1998) 131-40.
[20] R.W. Gale, Three-Compartment Model for Contaminant Accumulation by Semipermeable Membrane Devices, Environ. Sci. Technol., 32 (1998) 2292-2300. DOI: 10.1021/es970754m

[21] T.B. Boving and P. Grathwohl, Tracer diffusion coefficients in sedimentary rocks: correlation to porosity and hydraulic conductivity, J. of Contaminant Hydrology, 53 (2001) 83-100. DOI: 10.1016/S0169-7722(01)00138-3
[22] J.M.P.Q. Delgado, A critical review of dispersion in packed beds, Heat and Mass Transfer/Waerme- und Stoffuebertragung, 42 (2006) 279-310. DOI: 10.1007/s00231-005-0019-0
[23] G.E. Archie, The electrical resistivity log as an aid in determining some reservoir characteristics, Trans. Am. Inst. Mining Eng. , 146 (1942). DOI: 10.2118/942054-G
[24] G. H. Peterson, Sorption of water by vinyl polymers, Journal of Polymer Science, 28, 117 (1958) 458-459. DOI: 10.1002/pol.1958.1202811735
[25] H. Franquet-Griell, V. Pueyo, J. Silva, V. M. Orera, S. Lacorte, Development of a macroporous ceramic passive sampler for the monitoring of cytostatic drugs in water, Chemosphere 182 (2017) 681-690. DOI: 10.1016/j.chemosphere.2017.05.051.0045-6535.